Highly Polarizable Rydberg Ion in a Paul Trap

Gerard Higgins,[1,2,*] Fabian Pokorny,[1] Chi Zhang,[1] and Markus Hennrich[1]
[1]Department of Physics, Stockholm University, SE-106 91 Stockholm, Sweden
[2]Institut für Experimentalphysik, Universität Innsbruck, AT-6020 Innsbruck, Austria

(Received 18 April 2019; published 11 October 2019)

Usually the influence of the quadratic Stark effect on an ion's trapping potential is minuscule and only needs to be considered in atomic clock experiments. In this work we excite a trapped ion to a Rydberg state with polarizability ∼8 orders of magnitude higher than a low-lying electronic state; we find that the highly polarizable ion experiences a vastly different trapping potential owing to the Stark effect. We observe changes in trap stiffness, equilibrium position, and minimum potential, which can be tuned using the trapping electric fields. These effects lie at the heart of several proposed studies, including a high-fidelity submicrosecond entangling operation; in addition we demonstrate these effects may be used to minimize ion micromotion. Mitigation of Stark effects is important for coherent control of Rydberg ions; we illustrate this by carrying out the first Rabi oscillations between a low-lying electronic state and a Rydberg state of an ion.

DOI: 10.1103/PhysRevLett.123.153602

Although ions in Paul traps are confined close to an electric field minimum, they experience nonzero electric fields which modify the trapping potential via the quadratic Stark effect $\Delta U = -\frac{1}{2}\alpha\mathcal{E}^2$. While this modification is small for atomic ions in low-lying electronic (LLE) states, it strongly affects the trapping potential of highly polarizable Rydberg ions, causing striking phenomena to emerge when trapped ions are excited to Rydberg states.

Because the trap stiffness is modified by the Stark effect, atomic transition frequencies depend on motional phonon numbers and differential polarizabilities. This temperature-dependent Stark shift must be accounted for in trapped ion atomic clocks which operate below the 10^{-17} level [1–3]. We observe this effect directly for the first time by exciting an ion to a highly polarizable Rydberg state.

We find that a static offset electric field changes the equilibrium position and the minimum potential of the trapping potential of a highly polarizable Rydberg ion relative to that of an ion in a LLE state. The change in minimum potential alters the Rydberg-excitation energy; this shift may be used to reduce micromotion beyond the state-of-the-art level. Micromotion minimalization is critical for trapped ion atomic clocks [4,5] and for studies of atom-ion collisions in the quantum regime [6–8]. The change in trap position allows us to strongly drive phonon-number changing transitions during Rydberg excitation. The shifted trapping potential means our system may be used for studying quantum fluctuations of work [9,10] or for simulations of molecular dynamics [11].

Trapped Rydberg ions are an exciting new platform for quantum information processing [12], which combines the exquisite control of trapped ion systems with the strong interactions of Rydberg atoms. Stark effects must be mitigated for Rydberg ions to be coherently controlled; we illustrate this by driving the first Rabi oscillations between a LLE state and a Rydberg state of a trapped ion.

Numerous proposed studies rely on the change of trap stiffness during Rydberg excitation, including a high-fidelity submicrosecond entangling operation [13], vibrational mode shaping in large ion strings [14], coherent driving of structural phase transitions [11], and simulations of quantum magnetism [15] and the generalized Dicke model [16]. Here we lay the necessary experimental groundwork for realization of these proposals.

In a linear Paul trap ions are confined by a combination of oscillating and static electric quadrupole fields. When the null of the oscillating quadrupole field and the null of the static quadrupole field overlap, the electric potential near the center is

$$\Phi(t) = A\cos\Omega t(x^2 - y^2) - B[(1+\epsilon)x^2 + (1-\epsilon)y^2 - 2z^2]$$

where A and B are the electric field gradients of the oscillating and static electric quadrupole fields, Ω is the frequency of the oscillating field, and ϵ accounts for nondegeneracy of the radial trapping frequencies.

Although ions are dynamically trapped, the effective trapping potential can be described by the time-independent harmonic pseudopotential [17]

$$U = \frac{1}{2}M(\omega_x^2 x^2 + \omega_y^2 y^2 + \omega_z^2 z^2)$$

where M is the ion mass and the trapping frequencies $\omega_{x,y,z}$ depend on A, B, ϵ and Ω as described in Ref. [18].

A trapped ion with polarizability α experiences Stark shift $\Delta U = -\frac{1}{2}\alpha\mathcal{E}(t)^2$, where the electric field $\vec{\mathcal{E}}(t) = -\vec{\nabla}\Phi(t)$. When considering timescales much longer than the trap drive period $2\pi/\Omega$ the squared electric field strength can be time averaged and, provided $\Delta U \ll \hbar\Omega$, ΔU takes the form of an additional harmonic potential

$$\begin{aligned}\Delta U &= -\frac{1}{2}\alpha\langle\mathcal{E}(t)^2\rangle \\ &\approx -\alpha A^2(x^2+y^2)\end{aligned} \tag{1}$$

where the approximation uses $A^2 \gg B^2$, which is usually satisfied. A polarizable ion experiences altered trapping potential $U' = U + \Delta U$ with altered trapping frequencies

$$\omega_x' \approx \sqrt{\omega_x^2 - \frac{2\alpha A^2}{M}}, \qquad \omega_y' \approx \sqrt{\omega_y^2 - \frac{2\alpha A^2}{M}}, \qquad \omega_z' \approx \omega_z. \tag{2}$$

As a result, the transition frequency between two atomic states with polarizabilities $\{\alpha_1, \alpha_2\}$ depends on the number of phonons in radial motional modes $\{n_x, n_y\}$,

$$\begin{aligned}\Delta E_{1\to 2} = &\left(n_x + \frac{1}{2}\right)\hbar[\omega_x'(\alpha_2) - \omega_x'(\alpha_1)] \\ &+ \left(n_y + \frac{1}{2}\right)\hbar[\omega_y'(\alpha_2) - \omega_y'(\alpha_1)],\end{aligned} \tag{3}$$

as illustrated in Fig. 1(a). We confirm Eq. (3) experimentally as follows: We prepare a single trapped $^{88}Sr^+$ ion in number states of the radial modes and measure the dependence of the $4D_{5/2} \leftrightarrow 46S_{1/2}$ transition frequency on the radial phonon number using spectroscopy. Details about the preparation of phonon number states and the Rydberg detection scheme, as well as example Rydberg-excitation spectra, are in Ref. [18]. Results are shown in Fig. 1(b); the resonance frequency is displayed relative to the resonance frequency of an ion with zero radial phonons. The model line uses Eq. (3) with $\alpha_2 \equiv \alpha(46S_{1/2}) = 5.6 \times 10^{-31}\ \mathrm{C\,m^2\,V^{-1}}$ (given by theory [25]) and $\alpha_1 \equiv \alpha(4D_{5/2}) \approx 0$ [$\alpha(4D_{5/2})$ is 8 orders of magnitude smaller than $\alpha(46S_{1/2})$ [26] and is negligible in our experiments]. The energy shift in Eq. (3) results from the mean-squared electric field strength sampled by the polarizable ion during secular motion; inclusion of intrinsic micromotion changes the model prediction by ≈2% [18].

Because the transition frequency between states with different polarizabilities depends on phonon number, an ion with a broad radial phonon distribution will display a broader resonance linewidth than an ion with a narrow radial phonon distribution. As a result narrow radial phonon distributions and thus near-ground-state cooling is advantageous for trapped ion atomic clocks which operate below the 10^{-17} level. This effect was used to explain differences between the Rydberg-excitation spectral line shapes of a sideband-cooled ion and a Doppler-cooled ion in Ref. [27].

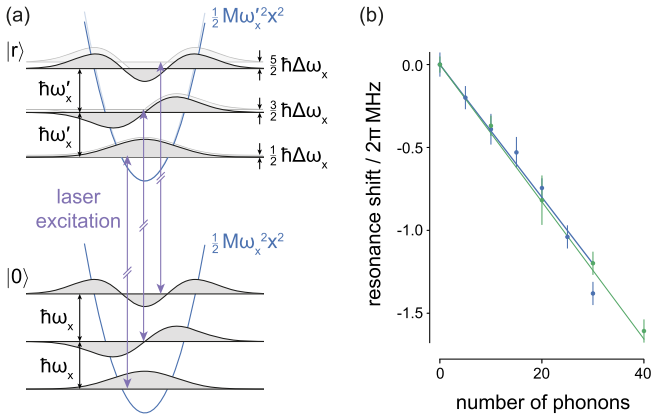

FIG. 1. Transition energy between two states with different polarizabilities depends on phonon number. (a) Illustration of the trapping potential and phonon states in the x direction for an ion in a LLE state with negligible polarizability $|0\rangle$ and a highly polarizable Rydberg state $|r\rangle$; $\Delta\omega_x = \omega_x' - \omega_x$. (b) The $4D_{5/2} \leftrightarrow 46S_{1/2}$ resonance frequency decreases as the number of phonons in the x mode (y mode) is increased while the number of phonons in the y mode (x mode) is fixed at 0; data points are blue (green). The theory lines use Eq. (3) with $\omega_x' - \omega_x = -2\pi \times 40.1$ kHz and $\omega_y' - \omega_y = -2\pi \times 41.4$ kHz. Error bars (68% confidence interval) are dominated by frequency drifts of the Rydberg-excitation lasers.

The quadratic Stark effect is manifest in a more striking fashion when the null of the static electric quadrupole field ($\vec{r}_{\mathrm{dc}}$) and the null of the oscillating electric quadrupole field ($\vec{r}_{\mathrm{rf}}$) do not overlap. In such a setup the ion equilibrium position depends on its polarizability; as a result phonon-number changing transitions may be strongly driven between states with different polarizabilities [12].

When a static electric field $\vec{\mathcal{E}}_{\mathrm{offset}} = (\mathcal{E}_{\mathrm{offset},x}, \mathcal{E}_{\mathrm{offset},y}, 0)$ is applied to the system the null of the static quadrupole field is shifted to $\vec{r}_{\mathrm{dc}} = (x_{\mathrm{dc}}, y_{\mathrm{dc}}, 0)$ where

$$x_{\mathrm{dc}} = -\frac{\mathcal{E}_{\mathrm{offset},x}}{2B(1+\epsilon)}, \qquad y_{\mathrm{dc}} = -\frac{\mathcal{E}_{\mathrm{offset},y}}{2B(1-\epsilon)},$$

while the null of the oscillating quadrupole field is unchanged $\vec{r}_{\mathrm{rf}} = (0, 0, z)$. The electric potential becomes

$$\begin{aligned}\Phi(t) = &A\cos\Omega t(x^2 - y^2) - B[(1+\epsilon)(x - x_{\mathrm{dc}})^2 \\ &+ (1-\epsilon)(y - y_{\mathrm{dc}})^2 - 2z^2]\end{aligned} \tag{4}$$

and the harmonic pseudopotential becomes [4]

$$U = \frac{1}{2}M(\omega_x^2(x - x_{\mathrm{eq}})^2 + \omega_y^2(y - y_{\mathrm{eq}})^2 + \omega_z^2 z^2)$$

where

$$x_{\mathrm{eq}} = \frac{e\mathcal{E}_{\mathrm{offset},x}}{M\omega_x^2}, \qquad y_{\mathrm{eq}} = \frac{e\mathcal{E}_{\mathrm{offset},y}}{M\omega_y^2}$$

and the equilibrium position $\vec{r}_{\mathrm{eq}} = (x_{\mathrm{eq}}, y_{\mathrm{eq}}, 0)$.

A polarizable ion experiences the additional harmonic potential ΔU from Eq. (1) and U' becomes

$$U' = \frac{1}{2}M(\omega_x'^2(x - x'_{\mathrm{eq}})^2 + \omega_y'^2(y - y'_{\mathrm{eq}})^2 + \omega_z{}^2 z^2) + \delta$$

where the equilibrium position is $\vec{r}'_{\mathrm{eq}} = (x'_{\mathrm{eq}}, y'_{\mathrm{eq}}, 0)$ with

$$x'_{\mathrm{eq}} = x_{\mathrm{eq}}\left(1 - \frac{2\alpha A^2}{M\omega_x^2}\right)^{-1}, \quad y'_{\mathrm{eq}} = y_{\mathrm{eq}}\left(1 - \frac{2\alpha A^2}{M\omega_y^2}\right)^{-1} \tag{5}$$

and the energy shift

$$\begin{aligned}\delta &= \frac{1}{2}M(\omega_x^2 x_{\mathrm{eq}}^2 + \omega_y^2 y_{\mathrm{eq}}^2 - \omega_x'^2 x'^2_{\mathrm{eq}} - \omega_y'^2 y'^2_{\mathrm{eq}}) \\ &\approx -\alpha A^2(x_{\mathrm{eq}}^2 + y_{\mathrm{eq}}^2) = -\frac{1}{2}\alpha\langle\mathcal{E}(\vec{r}_{\mathrm{eq}}, t)^2\rangle.\end{aligned} \tag{6}$$

The approximation in Eq. (6) reveals δ is a quadratic Stark shift which results from the electric field at the equilibrium position $\vec{r}_{\mathrm{eq}}$ acting on the polarizable ion. This approximation is valid provided $|\alpha A^2| \ll \frac{1}{2}M\omega_{x,y}^2$ such that the Stark shift ΔU can be treated as a perturbation. It is worth noting that although δ appears when there is excess micromotion in the system it does not result from this motion. The differences between U and U' are represented in Fig. 2(a).

We measure δ in the experiment: Our setup includes electrodes which we use to control $\vec{\mathcal{E}}_{\mathrm{offset}}$ to overlap the null of the oscillating quadrupole field and the null of the static quadrupole fields and thus minimize micromotion (schematic in Ref. [18]). We vary the voltage applied to one of these electrodes and measure a quadratic response of the $4D_{5/2} \leftrightarrow 46S_{1/2}$ resonance frequency, shown in Fig. 2(b). The x axis is rescaled to $\langle\mathcal{E}(r_{\mathrm{eq}}, t)^2\rangle$ [18] and we see the frequency shift obeys Eq. (6). This shift was observed previously in transitions between LLE states [28,29]; here the shift is several orders of magnitude larger owing to the giant Rydberg ion polarizability. The additional shift due to the altered trap stiffness in Eq. (3) is negligible here since sideband cooling is employed.

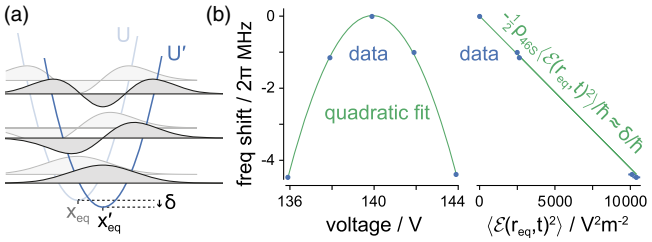

FIG. 2. The trapping potential of a polarizable ion is shifted when the null of the oscillating quadrupole field and the null of the static electric quadrupole field do not overlap. (a) Schematic. (b) Energy shift δ is measured: an offset field is varied via the voltage on an electrode and the Rydberg-excitation energy responds quadratically. The x axis is rescaled [18] to show the shift follows Eq. (6). Frequency drifts of the Rydberg-excitation lasers cause errors too small to be visible in this plot, x-error bars from uncertainty in x-axis rescaling are just discernible (68% confidence interval).

Excess micromotion vanishes at the turning point in Fig. 2(b); Rydberg spectroscopy may thus be used to minimize micromotion. We use this method to reduce the residual oscillating field strength at the equilibrium position $\vec{r}_{\mathrm{eq}}$ to $\mathcal{E}_{\mathrm{res}} \approx 20\ \mathrm{V\,m^{-1}}$. We expect this method will allow us to reduce the residual oscillating field strength beyond the state-of-the-art $\mathcal{E}_{\mathrm{res}} \approx 0.3\ \mathrm{V\,m^{-1}}$ level [5,30] after we improve the frequency stability of the Rydberg-excitation lasers and when we employ Rydberg states with higher polarizabilities [18]. This method has the advantage that it is sensitive to micromotion in all directions with a single probing setup. Stark shifts of neutral Rydberg atoms have already been used to minimize stray electric fields in neutral atom systems [31].

The differences between the trapping potentials in Fig. 2(a) are reminiscent of different vibronic potentials in molecules. Just as for molecular transitions, a transition from a LLE state to a Rydberg state involves a change of the motional state and the transition moment depends on the overlap integral of the motional states (Franck-Condon factor). Transitions in which the phonon numbers change may be driven strongly when the trapping potentials significantly differ $(n_x|\omega_x' - \omega_x| \ll \omega_x$ or $\sqrt{n_x}|x'_{\mathrm{eq}} - x_{\mathrm{eq}}| \ll x_{\mathrm{ho}}$, where x_{ho} is the characteristic length of the harmonic oscillator).

We experimentally investigate these strong phonon-number changing transitions as follows: We prepare a single ion in motional state $n_x = 20$, $n_y = 0$ and measure Rydberg-excitation spectra as we vary $|\vec{r}_{\mathrm{eq}} - \vec{r}'_{\mathrm{eq}}|$ by controlling an offset electric field via a micromotion-minimization electrode (schematic in Ref. [18]). The results are shown in Fig. 3. The peak at zero laser detuning corresponds to the phonon-number preserving transition, while peaks at laser detuning $N \times \omega_x'$ correspond to phonon-number changing transitions $n_x \to n_x' = n_x + N$ (since $n_x \gg n_y$ the phonon-number changing transitions are dominated by the x mode). From (a) $\to$ (c) $|x_{\mathrm{eq}} - x'_{\mathrm{eq}}|$ increases and phonon-number changing transitions are driven more strongly. Reasonable quantitative agreement is observed between experimental data and model curves in which the heights of resonance peaks are given by the overlap integrals $\langle n_x|n_x'\rangle$. The model curves use experimentally constrained parameters (details in Ref. [18]).

Phonon-number changing transitions also arise in trapped ion experiments due to laser phase gradients [18,32] or due to magnetic field gradients [33–35]; here this phenomenon is made possible due to the Stark effect.

Franck-Condon factors are ubiquitous in transitions between molecular vibronic states, and thus trapped Rydberg ions may serve as a natural system for quantum simulation of molecular systems [11]. The difference between the trapping potentials U and U' may also allow quantum fluctuations of work to be investigated [9,10].

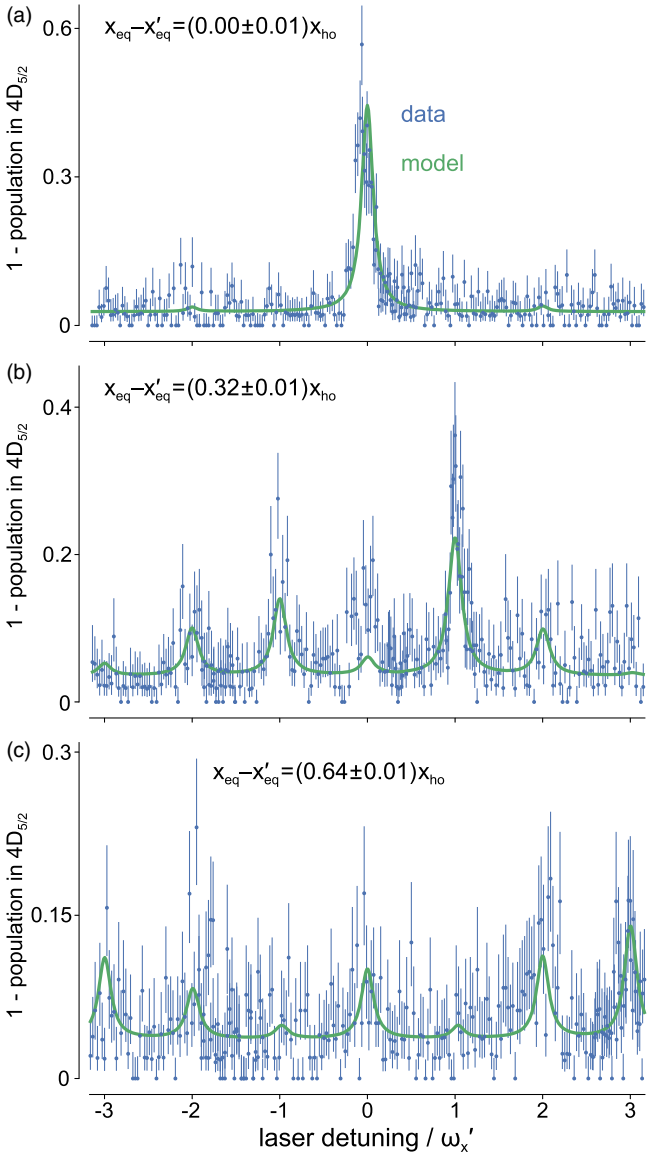

FIG. 3. The ion's motional state can be changed during a transition between electronic states with different polarizabilities. Rydberg-excitation spectra for an ion prepared with $n_x = 20$ and $n_y = 0$. Resonances at laser detuning $N \times \omega'_x$ correspond to transitions which increase the phonon number by N. From (a) → (c) $|x_{eq} - x'_{eq}|$ is increased (by controlling an offset electric field $\vec{\mathcal{E}}_{offset}$) and phonon-number changing transitions are driven more strongly. x_{ho} is the harmonic oscillator characteristic length. The spectra are modeled [18] by Lorentzian absorption lines separated by ω'_x with amplitudes given by the overlap integrals of the phonon states. The model curves use only experimentally constrained parameters. Error bars indicate projection noise (68% confidence interval).

Because $\mathcal{E}(t)$ oscillates with frequency Ω the quadratic Stark shift oscillates with frequency 2Ω and sidebands appear in excitation spectra at even multiples of Ω, provided $\alpha\langle\mathcal{E}(t)^2\rangle/2 \ll \hbar(2\Omega)$. These Stark sidebands are distinct from the usual micromotion sidebands described by the first-order Doppler effect [4]. Stark sidebands are used to describe spectral line shapes in another Rydberg ion experiment [36,37]. In our system $\alpha\langle\mathcal{E}^2\rangle/2 \ll \hbar(2\Omega)$ and Stark sidebands are not observed.

Just as with high-precision trapped ion atomic clocks, quantum information processing with Rydberg ions requires mitigation of the quadratic Stark effect, since high-fidelity operations require addressing individual narrow transition lines. Stark effects may be mitigated by using microwave-dressed Rydberg states with vanishing polarizabilities [38] (cf. ideal clock transitions have small differential polarizabilities [39]); alternatively $\langle\mathcal{E}^2\rangle$ may be minimized by ground-state cooling of radial motional modes and by overlapping the null of the oscillating quadrupole field and the null of the static quadrupole field (i.e., micromotion minimization).

We illustrate the importance of mitigating the quadratic Stark effect by comparing Rabi oscillations between LLE state $4D_{5/2}$ and Rydberg state $46S_{1/2}$ for a sideband-cooled ion (with a narrow radial phonon distribution) and a Doppler-cooled ion (with a broad radial phonon distribution) in Fig. 4: Rabi oscillations are visible for the sideband-cooled ion, while they are smeared out for the Doppler-cooled ion owing to its broader resonance linewidth which stems from Eq. (3). The parameters of the theory curves are experimentally constrained, as described in Ref. [18]. Although coherent excitation of a Rydberg ion

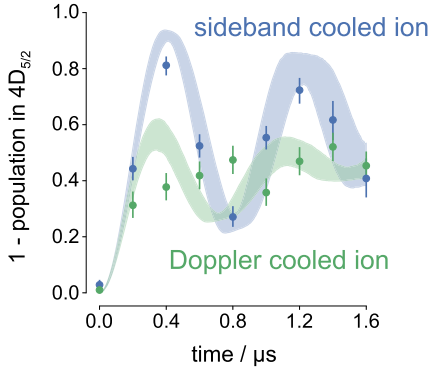

FIG. 4. Rabi oscillations between LLE state $4D_{5/2}$ and Rydberg state $46S_{1/2}$ are observed when radial sideband cooling is employed, while oscillations are washed out when a warmer Doppler-cooled ion is used. Error bars indicate projection noise (68% confidence interval) and shaded areas show the central 68% of the Monte Carlo simulation results [18].

using stimulated Raman adiabatic passage was demonstrated in Ref. [40], this work is the first to demonstrate Rabi oscillations between a LLE state and a Rydberg state. Such coherent excitation is required for a two-qubit gate using Rydberg-blockade [41] as was realized with neutral atoms [42].

In summary we use a highly polarizable ion to investigate the influence of the Stark effect on an ion's trapping potential. This work is a milestone towards realization of quantum information processing using strongly interacting Rydberg ions [12] and it provides a solid basis for a range of proposed studies which rely on the altered trapping potential of Rydberg ions [11,14–16] including a high-fidelity submicrosecond entangling operation [13].

We thank Weibin Li for theory values of Rydberg state polarizabilities, Tanja Mehlstäubler for discussions, and Jonas Vogel for assistance in the laboratory. This work was supported by the European Research Council under the European Union's Seventh Framework Programme/ERC Grant Agreement No. 279508, the Swedish Research Council (Trapped Rydberg Ion Quantum Simulator), the QuantERA ERA-NET Cofund in Quantum Technologies implemented within the European Union's Horizon 2020 Programme (ERyQSenS), and the Knut & Alice Wallenberg Foundation ("Photonic Quantum Information" and WACQT).

*gerard.higgins@fysik.su.se

[1] C. W. Chou, D. B. Hume, J. C. J. Koelemeij, D. J. Wineland, and T. Rosenband, Phys. Rev. Lett. **104**, 070802 (2010).
[2] C. Sanner, N. Huntemann, R. Lange, C. Tamm, E. Peik, M. S. Safronova, and S. G. Porsev, Nature (London) **567**, 204 (2019).
[3] S. M. Brewer, J.-S. Chen, A. M. Hankin, E. R. Clements, C. W. Chou, D. J. Wineland, D. B. Hume, and D. R. Leibrandt, Phys. Rev. Lett. **123**, 033201 (2019).
[4] D. J. Berkeland, J. D. Miller, J. C. Bergquist, W. M. Itano, and D. J. Wineland, J. Appl. Phys. **83**, 5025 (1998).
[5] J. Keller, H. L. Partner, T. Burgermeister, and T. E. Mehlstäubler, J. Appl. Phys. **118**, 104501 (2015).
[6] A. T. Grier, M. Cetina, F. Oručević, and V. Vuletić, Phys. Rev. Lett. **102**, 223201 (2009).
[7] S. Schmid, A. Härter, and J. H. Denschlag, Phys. Rev. Lett. **105**, 133202 (2010).
[8] C. Zipkes, S. Palzer, C. Sias, and M. Köhl, Nature (London) **464**, 388 (2010).
[9] G. Huber, F. Schmidt-Kaler, S. Deffner, and E. Lutz, Phys. Rev. Lett. **101**, 070403 (2008).
[10] S. An, J.-N. Zhang, M. Um, D. Lv, Y. Lu, J. Zhang, Z.-Q. Yin, H. T. Quan, and K. Kim, Nat. Phys. **11**, 193 (2015).
[11] W. Li and I. Lesanovsky, Phys. Rev. Lett. **108**, 023003 (2012).
[12] M. Müller, L. Liang, I. Lesanovsky, and P. Zoller, New J. Phys. **10**, 093009 (2008).
[13] J. Vogel, W. Li, A. Mokhberi, I. Lesanovsky, and F. Schmidt-Kaler, following Letter, Phys. Rev. Lett. **123**, 153603 (2019).
[14] W. Li, A. W. Glaetzle, R. Nath, and I. Lesanovsky, Phys. Rev. A **87**, 052304 (2013).
[15] R. Nath, M. Dalmonte, A. W. Glaetzle, P. Zoller, F. Schmidt-Kaler, and R. Gerritsma, New J. Phys. **17**, 065018 (2015).
[16] F. M. Gambetta, I. Lesanovsky, and W. Li, Phys. Rev. A **100**, 022513 (2019).
[17] F. G. Major, V. N. Gheorghe, and G. Werth, *Charged Particle Traps* (Springer-Verlag, Berlin Heidelberg, 2005).
[18] See Supplemental Material at http://link.aps.org/supplemental/10.1103/PhysRevLett.123.153602 for more details. Lasers used, detection of Rydberg excitation, trap electrodes, example spectra, effective Lamb-Dicke parameter, relationship between field gradients and trapping frequencies, effect of micromotion on Stark shifts, rescaling of x axis in Fig. 2, model in Fig. 3, constraints of model parameters in Fig. 3, and Fig. 4, method to prepare phonon-number states, simulation results in Fig. 4, limits of micromotion compensation using Rydberg spectroscopy, and it includes Refs. [19–24].
[19] H. Zhang, M. Gutierrez, G. H. Low, R. Rines, J. Stuart, T. Wu, and I. Chuang, New J. Phys. **18**, 123021 (2016).
[20] U. I. Safronova, Phys. Rev. A **82**, 022504 (2010).
[21] D. Leibfried, R. Blatt, C. Monroe, and D. Wineland, Rev. Mod. Phys. **75**, 281 (2003).
[22] D. James, Appl. Phys. B **66**, 181 (1998).
[23] D. M. Meekhof, C. Monroe, B. E. King, W. M. Itano, and D. J. Wineland, Phys. Rev. Lett. **76**, 1796 (1996).
[24] J. Johansson, P. Nation, and F. Nori, Comput. Phys. Commun. **184**, 1234 (2013).
[25] W. Li (private communication).
[26] D. Jiang, B. Arora, M. S. Safronova, and C. W. Clark, J. Phys. B **42**, 154020 (2009).
[27] G. Higgins, W. Li, F. Pokorny, C. Zhang, F. Kress, C. Maier, J. Haag, Q. Bodart, I. Lesanovsky, and M. Hennrich, Phys. Rev. X **7**, 021038 (2017).
[28] N. Yu, X. Zhao, H. Dehmelt, and W. Nagourney, Phys. Rev. A **50**, 2738 (1994).
[29] T. Schneider, E. Peik, and C. Tamm, Phys. Rev. Lett. **94**, 230801 (2005).
[30] A. Härter, A. Krükow, A. Brunner, and J. Hecker Denschlag, Appl. Phys. Lett. **102**, 221115 (2013).
[31] A. Osterwalder and F. Merkt, Phys. Rev. Lett. **82**, 1831 (1999).
[32] D. J. Wineland, C. Monroe, W. M. Itano, D. Leibfried, B. E. King, and D. M. Meekhof, J. Res. Natl. Inst. Stand. Technol. **103**, 259 (1998).
[33] C. Ospelkaus, C. E. Langer, J. M. Amini, K. R. Brown, D. Leibfried, and D. J. Wineland, Phys. Rev. Lett. **101**, 090502 (2008).
[34] M. Johanning, A. Braun, N. Timoney, V. Elman, W. Neuhauser, and C. Wunderlich, Phys. Rev. Lett. **102**, 073004 (2009).
[35] R. Srinivas, S. C. Burd, R. T. Sutherland, A. C. Wilson, D. J. Wineland, D. Leibfried, D. T. C. Allcock, and D. H. Slichter, Phys. Rev. Lett. **122**, 163201 (2019).
[36] T. Feldker, P. Bachor, M. Stappel, D. Kolbe, R. Gerritsma, J. Walz, and F. Schmidt-Kaler, Phys. Rev. Lett. **115**, 173001 (2015).
[37] A. Mokhberi, J. Vogel, J. Andrijauskas, P. Bachor, J. Walz, and F. Schmidt-Kaler, arXiv:1902.04391.

[38] W. Li and I. Lesanovsky, Appl. Phys. B **114**, 37 (2014).
[39] A. D. Ludlow, M. M. Boyd, J. Ye, E. Peik, and P. O. Schmidt, Rev. Mod. Phys. **87**, 637 (2015).
[40] G. Higgins, F. Pokorny, C. Zhang, Q. Bodart, and M. Hennrich, Phys. Rev. Lett. **119**, 220501 (2017).
[41] D. Jaksch, J. I. Cirac, P. Zoller, S. L. Rolston, R. Côté, and M. D. Lukin, Phys. Rev. Lett. **85**, 2208 (2000).
[42] L. Isenhower, E. Urban, X. L. Zhang, A. T. Gill, T. Henage, T. A. Johnson, T. G. Walker, and M. Saffman, Phys. Rev. Lett. **104**, 010503 (2010).